

Aromaticity of Benzene in the Facial Coordination Mode: A Structural and Theoretical Study**

Hubert Wadepohl* and Maria Entrialgo Castaño^[a]

Abstract: The effects of facial coordination of benzene to a trinuclear transition-metal cluster have been studied by structure correlation and DFT calculational methods. Data taken from the X-ray crystal structures of twelve complexes $[(\eta\text{-C}_5\text{H}_4\text{R}'')\text{Co}]_3(\mu_3\text{-}\eta^2\text{:}\eta^2\text{:}\eta^2\text{-C}_6\text{H}_4\text{RR}')$ **1b–1m** were analyzed by using standard statistical methods. The prototypal facial arene ligand is considerably expanded with respect to free benzene and shows a small but highly

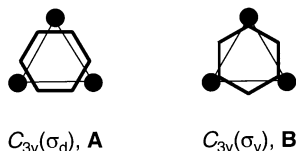
significant Kekulé distortion ($d_{\text{CC}} = 1.42, 1.45 \text{ \AA}$). DFT MO calculations were carried out on the model complexes $[(\eta\text{-C}_5\text{H}_5)\text{M}]_3(\mu\text{-}\eta^2\text{:}\eta^2\text{:}\eta^2\text{-C}_6\text{H}_6)$ **1a** ($\text{M} = \text{Co}$), **2** ($\text{M} = \text{Rh}$), and **3** ($\text{M} = \text{Ir}$). Ring currents in the facial benzene and

apical cyclopentadienyl ligands have been assessed by nucleus independent chemical shift (NICS) calculations. Compared to the free ligand (with the optimized D_{6h} structure as well as with D_{3h} and a C_{3v} geometries similar to that in the prototypal facial arene), facial benzene exhibits somewhat reduced but still substantial cyclic electron delocalization (CED). The calculated order of CED is benzene $\sim [(\text{CO})_3\text{Cr}(\eta\text{-C}_6\text{H}_6)]$ **4** > **1** > **2** > **3**.

Keywords: arene ligands • aromaticity • cluster compounds • density functional calculations • structure correlation

Introduction

Among the many known metal complexes of benzene and its substituted derivatives those with a facial (μ_3 -) coordination of the arene ring to a triangular array of metals form a distinct and structurally well characterized class.^[2] The wide scope of such systems is marked by the extremes of adsorption states on metal surfaces on the one hand, and trinuclear molecular cluster complexes on the other. In the molecular systems, the staggered ($C_{3v}(\sigma_d)$, **A**) orientation of the M_3 and C_6 rings is preferred to the eclipsed ($C_{3v}(\sigma_v)$, **B**) alternative, with so far only one notable exception.^[3] The situation is less clear cut on close-packed metal surfaces, where other (on-top, C_{6v} and bridge, C_{2v}) coordination sites also play a role.^[4]



The geometry of benzene in $C_{3v}(\sigma_d)$ surface adsorption sites, in particular a possible trigonal in-plane (Kekulé-type) distortion, has been addressed by many surface structural

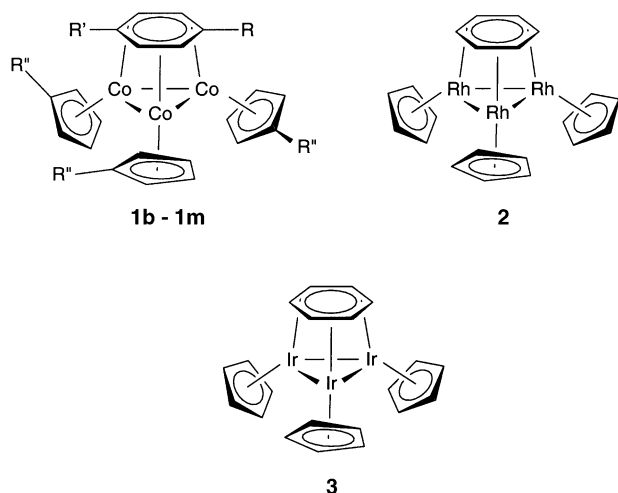
studies. An alternating lengthening and shortening of the C–C bonds would result in the formation of the elusive cyclohexatriene, or Kekulé benzene, with a potential loss of aromaticity. However, due to the difficulties in obtaining reliable geometries of adsorbed molecules,^[5] no definitive conclusion has as yet been reached. Even on the same adsorption phases, contradictory results were reported from investigations carried out with different methods. For example, in the coadsorbate $\text{Rh}(111) - (3 \times 3) - (\text{C}_6\text{H}_6 + 2\text{CO})$, a strong Kekulé distortion ($d_{\text{CC}} = 1.33(15), 1.81(15) \text{ \AA}$) was found by using electron diffraction (LEED), while photoelectron spectroscopy (ARUPS) indicated an essentially undistorted hexagonal structure of the chemisorbed benzene.^[6]

In the molecular cluster regime, geometrical structures can be established with much higher precision due to the applicability of high-resolution single-crystal X-ray and neutron diffraction methods. A considerable number of cluster complexes with facial arene ligands have been structurally characterized.^[2,3] Based on such data, facial benzene ligands in ruthenium and osmium cluster complexes were occasionally regarded as trienes, because of a certain degree of C–C bond length alternation.^[7] General conclusions are however difficult to draw from any individual structure. In a particular complex, the structure of the facial benzene ligand could be influenced by deviations from the ideal symmetry of its coordination site. In addition, the facial arene can itself be asymmetric, for example due to the presence of substituents.

[a] Prof. Dr. H. Wadepohl, Lic. Quím. M. Entrialgo Castaño
Anorganisch-chemisches Institut der Ruprecht-Karls-Universität
Im Neuenheimer Feld 270, 69120 Heidelberg (Germany)
E-mail: bu9@ix.urz.uni-heidelberg.de

[**] Organometallic Cluster Complexes with Face-Capping Arene Ligands, Part 11. For Part 10: See reference [1].

Here we report a structural study with a class of organo-metallic μ_3 -arene cluster complexes, the family of tricobalt complexes $[\{(\eta\text{-C}_5\text{R}_5)\text{Co}\}_3(\mu_3\text{-arene})]$ **1**. Along with the statistical evaluation of observed Kekulé-type distortions of the facial benzene derivative, an attempt will be made to quantify a possible diminution of cyclic electron delocalization using the nucleus-independent cyclic chemical shift (NICS) criterium, obtained from first-principles MO calculations on the model complexes $[\{(\eta\text{-C}_5\text{H}_5)\text{M}\}_3(\mu_3\text{-benzene})]$ **1a** (M = Co), **2** (M = Rh) and **3** (M = Ir).



Experimental Section

Statistical analysis of the structural data was based on published algorithms.^[8] All Hartree–Fock (HF) and density functional theory^[9] (DFT) MO calculations were carried out with Gaussian98 using the standard basis sets supplied with this package (for details see next section).^[10] The structures of $[\{(\eta\text{-C}_5\text{H}_5)\text{M}\}_3(\mu_3\text{-C}_6\text{H}_6)]$ **1a** (M = Co), **2** (M = Rh) and **3** (M = Ir) were optimized at the B3LYP/LANL2DZ + ECP (small-effective-core potential)^[11] level, starting from a staggered $C_{3v}(\sigma_d)$ -like structure, with the constraint of overall C_3 molecular symmetry. The optimized structures were shown by frequency calculations to be true energy minima. NICS indices were obtained from HF or DFT GIAO calculations.^[12]

Results and Discussion

Analysis of crystal structure data; definition of the prototypical molecule: Known molecular cluster complexes with facial benzene or substituted benzene ligands fall into only a few categories. The metal frames may be an oligonuclear carbonyl metal $M_n(\text{CO})_m$ (M mainly Ru or Os) or cyclopentadienyl metal $M_3(\eta\text{-C}_5\text{R}_5)_3$ (M = Ru, Co, Rh) fragment. For our study we chose a series of tricobalt complexes of the type $[\{(\eta\text{-C}_5\text{H}_4\text{R})\text{Co}\}_3(\mu_3\text{-arene})]$ **1**.^[13] Our choice was based on the accuracy of the structural parameters, due to the presence of only first-row transition metals, and on a reasonable population of our sample, which is of paramount importance for any statistical analysis. Unfortunately, in all known derivatives of **1** the facial arene is invariably an alkyl- or alkenylbenzene derivative, which, in a very few cases, also has another

substituent on the metal coordinated phenyl ring. We therefore have to abstract from the particular derivatives to a (hypothetical) prototypical molecule $[\{(\eta\text{-C}_5\text{H}_5)\text{Co}\}_3(\mu_3\text{-arene})]$, which reflects the structural features common to all real derivatives.

Data from twelve crystal structure determinations were used in our analysis (Table 1). In the language of sampling theory,^[14] the population of all possible complexes of the type **1** is sampled by a limited number of structure determinations. In our dataset, the lengths of the endocyclic C–C bonds in the facial arenes range from 1.388 to 1.470 Å. The distribution appears fairly normal (Figure 1).

Table 1. Complexes of the type $[\{(\eta\text{-C}_5\text{H}_4\text{R})\text{Co}\}_3(\mu_3\text{-}\eta^2\text{:}\eta^2\text{:}\eta^2\text{-arene})]$ **1**.

| | R | Arene | T [K] | Ref code ^[a] |
|--------------------------|----|---------------------------------|-------|-------------------------|
| 1b | H | β -methylstyrene | amb. | GEHZIC |
| 1c | Me | β -methylstyrene | 203 | [b] |
| 1d | H | p -F- β -methylstyrene | 200 | FEBLIH |
| 1e | H | p -F- α -methylstyrene | amb. | TEZFOT |
| 1f | H | p -F- α -methylstyrene | 200 | [c] |
| 1g | H | 1,1-diphenylethene | amb. | KIRWEL |
| 1h | H | 1,1-diphenylethane | amb. | HIPKUM |
| 1i ^[d] | H | 1,1-diphenylethane | amb. | REPYEQ |
| 1j | H | 1,2-diphenylethane | amb. | HIPLAT |
| 1k | Me | 1,2-diphenylethane | 203 | [b] |
| 1l | H | 2-phenyl-butene-2 | amb. | FEBNOP |
| 1m | H | p -distyryldurene | 200 | [c] |

[a] CSD version 5.23, Cambridge Crystallographic Data Centre, 2002. [b] H. Wadepohl, A. Metz, H. Pritzkow, unpublished results. [c] H. Wadepohl, T. Borchert, H. Pritzkow, unpublished results. [d] $[\{(\eta\text{-C}_5\text{H}_5)\text{Co}\}_3(\mu_3\text{-H})(\mu_3\text{-}\eta^2\text{:}\eta^2\text{:}\eta^2\text{-arene})]^+$.

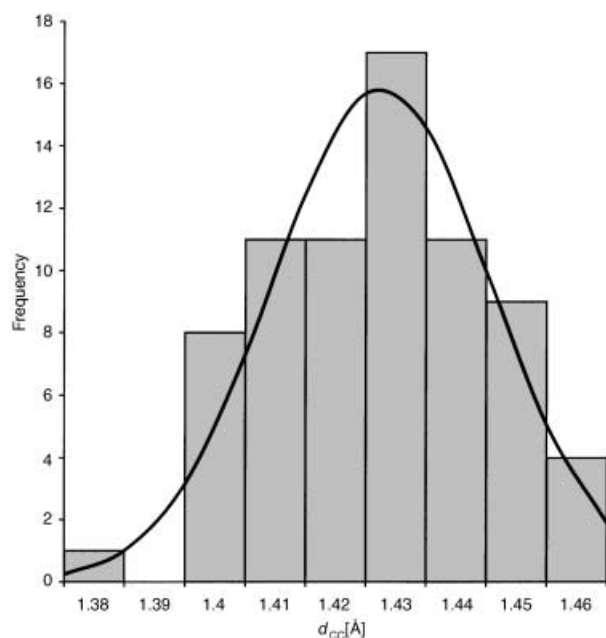


Figure 1. Distributions of all endocyclic C–C bond lengths in twelve cluster complexes of the type $[\{(\eta\text{-C}_5\text{H}_4\text{R})\text{Co}\}_3(\mu_3\text{-}\eta^2\text{:}\eta^2\text{:}\eta^2\text{-arene})]$ **1**.

This is confirmed by a normal probability plot^[15] (Figure 2) and the Shapiro–Wilk statistical test,^[16] which gives < 1% probability for the rejection of normality. However, for the

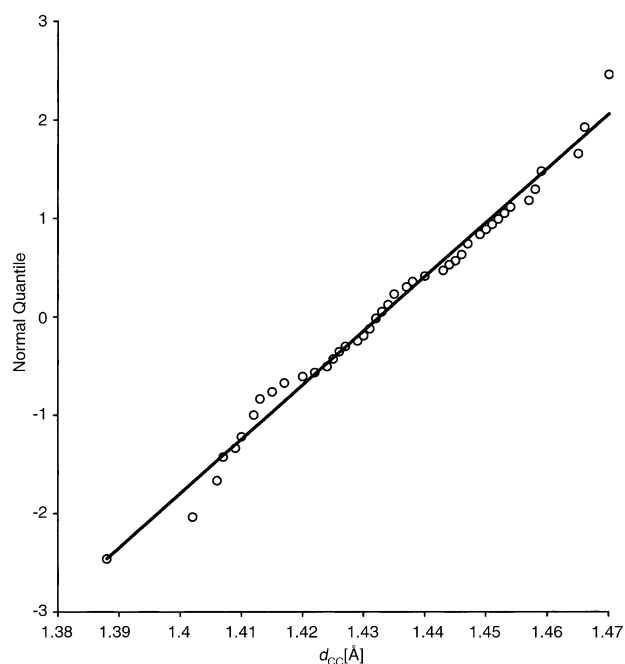


Figure 2. Normal probability plot of the data of Figure 1.

moment disregarding the substituent(s) on the facial arene ring, the threefold symmetry of the coordination site **A** results in two sets of ring C–C bonds, those 'on top' of the metal atoms and the noncoordinated bonds 'in between' the metals. Visualization of the respective bond lengths in histogram form (Figure 3) reveals an apparent difference between the two groups, the first group of bonds being somewhat shorter than

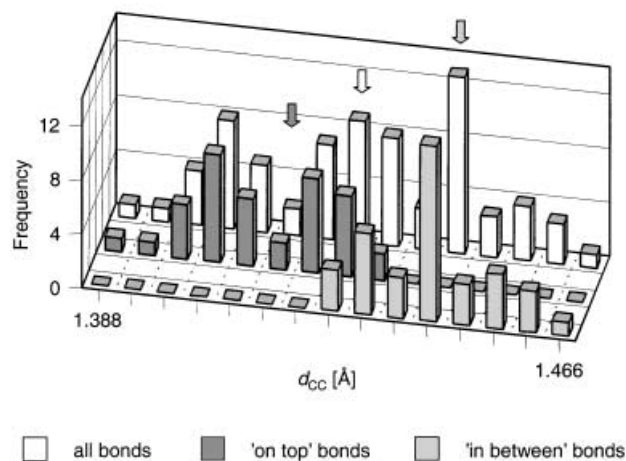


Figure 3. Dissected distributions of the endocyclic C–C bond lengths in twelve cluster complexes of the type $[(\eta\text{-C}_3\text{H}_4\text{R})\text{Co}]_3(\mu_3\text{-}\eta^2\text{:}\eta^2\text{:}\eta^2\text{-arene})$ **1**. Sampling intervals are 0.005 Å in the range 1.388–1.466 Å. The solid arrows indicate d_{mean} ('on top' bonds), d_{mean} (all bonds) and d_{mean} ('in between' bonds), respectively.

the second. However, with comparatively small samples such as ours, histograms (bar charts) can be misleading and are often considerably biased by the chosen range of values for any particular bar (compare Figures 1 and 3). In addition, considerable overlap of the two groups around $d_{\text{CC}} \approx 1.43$ Å is obvious from Figure 3.

Before venturing a detailed statistical analysis, we shall consider possible systematic bias of the data. Some of the structures (5 out of 12) were determined at low temperature (around 200 K). The structure of $[(\eta\text{-C}_3\text{H}_5)\text{Co}]_3(\mu_3\text{-}p\text{-F-}\beta\text{-methylstyrene})$, which has been obtained both from ambient and low temperature data, permits assessment of the effect of temperature. As expected, the standard deviations σ of the unit cell and atomic parameters are smaller for the low temperature structure. Relevant C–C bonds differ in length by 0.002–0.017 Å between the two structures (mean absolute difference 0.008 Å). With the maximum deviation being approximately $2\sigma_{\text{max}}(d_{\text{CC}})$, and the mean deviation well below this value, a systematic effect of data collection temperature was considered negligible, and hence no distinction was made between ambient and low-temperature data.

All the arene ligands in **1b–1m** are mono- or disubstituted benzene derivatives. The influence of substituents on the ring geometry of benzene derivatives has been investigated in some detail.^[17] The effects on the endocyclic C–C bond lengths was found to be quite small, and barely noticeable mainly in the bonds originating from the substituted ring carbon atom. In the $\mu_3\text{-}\eta^2\text{:}\eta^2\text{:}\eta^2$ coordinated ligand these belong to either of the two groups ('on top' and 'in between') defined above. Any systematic variation of these bonds would therefore primarily increase the scatter of the data.

Small modifications of the triscyclopentadienylcobalt frame (a methyl group on each of the cyclopentadienyl rings, or protonation of the Co_3 cluster; both modifications of the basic structure narrowing somewhat the coordination site of the facial arene) may be studied with the pairs of complexes (**1j**, **1k**), (**1b**, **1c**) and (**1h**, **1i**), respectively. Again, as far as the C–C bond lengths are concerned, no systematic pattern shows in the small deviations (complexes **1b** and **1c**, $\Delta d_{\text{CC}} = 0.003\text{--}0.012$ Å, $|\Delta d_{\text{CC}}|_{\text{mean}} = 0.010$ Å, $\sigma(d_{\text{CC}}) = 0.003\text{--}0.005$ Å; complexes **1j** and **1k**, $\Delta d_{\text{CC}} = 0.002\text{--}0.021$ Å, $|\Delta d_{\text{CC}}|_{\text{mean}} = 0.010$ Å, $\sigma(d_{\text{CC}}) = 0.004\text{--}0.008$ Å; complexes **1h** and **1i**, $\Delta d_{\text{CC}} = 0.003\text{--}0.019$ Å, $|\Delta d_{\text{CC}}|_{\text{mean}} = 0.009$ Å, $\sigma(d_{\text{CC}}) = 0.006\text{--}0.010$ Å). We therefore conclude that the observed distribution of the C–C bond lengths in facial arenes (Figure 3) is essentially due to intrinsic factors of this coordination mode, overlaid by smaller effects of different substituents and molecular packing in the crystals.

Statistical parameters relevant to our data are collected in Table 2. To account for the variable accuracy of the structures, weights proportional to $(1.5\sigma_{\text{bond}})^{-2}$ were applied, where σ_{bond}

Table 2. Prototypal bond lengths [Å] and relevant statistical data derived from the complexes $[(\eta\text{-C}_3\text{H}_4\text{R})\text{Co}]_3(\mu_3\text{-}\eta^2\text{:}\eta^2\text{:}\eta^2\text{-arene})$ **1b–m**.

| Type | n_{obs} | Median | Mean(σ_{mean}) | Weighted mean($\sigma_{\text{weighted mean}}$) | σ_{sample} | χ^2 | W, $p^{[a]}$ |
|------------------------|------------------|--------|--------------------------------|--|--------------------------|----------|--------------|
| $\eta\text{-CC}^{[b]}$ | 36 | 1.417 | 1.418(0.0018) | 1.420(0.0016) | 0.011 | 65.1 | 0.950, 0.14 |
| $\text{CC}^{[c]}$ | 36 | 1.447 | 1.447(0.0018) | 1.448(0.0017) | 0.011 | 67.0 | 0.948, 0.12 |
| all CC | 72 | 1.432 | 1.433(0.0021) | 1.434(0.0020) | 0.018 | 395.6 | 0.973, 0.35 |

[a] Shapiro–Wilk coefficient, significance probability p . [b] 'On top' bonds. [c] 'In between' bonds.

is the standard deviation of any individual bond. The factor of 1.5 was used to correct for the fact that standard deviations of bond lengths obtained from least squares refinement of X-ray diffraction data (“esds”) are generally systematically underestimated.^[18] In Table 2, the six C–C bonds of every μ_3 -arene ligand have been partitioned into two groups, those ‘on top’ (usually shorter) and those ‘in between’ the metals (usually longer). To be able to apply statistical significance tests, we have to assume an essentially normal distribution of our *populations*, that is the lengths of ‘on top’ and ‘in between’, respectively, C–C bonds in all possible complexes of type **1**. From what has been discussed above we are confident that this is actually the case. Our view is corroborated by normal probability plots (essentially linear) and by Shapiro–Wilk testing of the samples. Note that, since we are sampling these total populations with a rather limited number of crystal structures, the assumption of normality is not necessarily true (nor does it have to be true) for our *samples*,^[14] that is the determined values of the respective bond lengths.

We wish to establish if there is a real, statistically significant, Kekulé distortion in the typical facial arene ring. Hence, the null hypothesis we have to test for is whether or not the mean length of the ‘on top’ bonds is significantly different from that of the ‘in between’ bonds.^[19] As a more stringent condition, a difference between the means implies that the two samples are indeed taken from two different populations. Application of Student’s *t* test gives 99% confidence intervals of 1.415–1.424 Å and 1.442–1.452 Å, respectively, for the weighted means of our two samples, clearly indicative of a small but nevertheless highly significant difference. This bond length alternation by approximately 0.03 Å quantifies the Kekulé distortion of the prototypal arene ring when coordinated to a triscyclopentadienylcobalt cluster in the facial mode.

Molecular orbital calculations: Having established the significance of the experimentally-observed Kekulé distortion we now proceed to theoretical calculations on model complexes. For the sake of computational efficiency and ease of interpretation, the most simple derivatives, $[(\eta\text{-C}_5\text{H}_5)\text{M}]_3(\mu_3\text{-}\eta^2\text{:}\eta^2\text{:}\eta^2\text{-C}_6\text{H}_6)$ **1a** (M = Co) **2** (M = Rh) and **3** (M = Ir) were studied. Only one of these, complex **2** (M = Rh), has actually been prepared and structurally characterized.^[20]

Geometries and energies: Geometry optimizations of the cluster complexes were performed using DFT MO calcula-

tions. Our choice of basis set is discussed below, and details are given in the Experimental Section. A comparison of experimental and calculated structural parameters is compiled in Table 3. With the exception of the Co–Co bonds, calculated bond distances in the complexes **1a** and **2** are slightly longer (by 0.02–0.03 Å for the bonds which involve at least one metal) than in the crystal structures. The difference is smaller for the C–C bonds of the facial benzene (in the order of 0.01–0.02 Å). The salient features common to the minimum structures may be summarized as follows: i) a staggered, $C_{3v}(\sigma_d)$ arrangement of the Co_3 and facial C_6 rings is attained, ii) the facial benzene ligands are substantially expanded with a small Kekulé distortion ($\Delta d \approx 0.02$ Å for **1a**; 0.03 Å for **2** and **3**), and iii) the hydrogen substituents on the μ_3 -benzene are bent out of the ring plane by 16° (**1a**, **2**) and 20° (**3**), away from the metal cluster. An explanation of these effects has been given previously,^[21] based on simple frontier orbital arguments and approximate (Fenske–Hall) MO calculations, and need not be reiterated here. Differences of the electronic structures between derivatives with saturated and unsaturated side-chains, respectively, on the μ_3 -arene have also been examined and discussed earlier.^[22] They do not affect the bonding between the facial arene and the Co_3 cluster.

The energetics of the Kekulé-type in-plane and C–H out-of-plane bending distortions of free benzene are illustrated in Figure 4. It is interesting to note that expansion of the

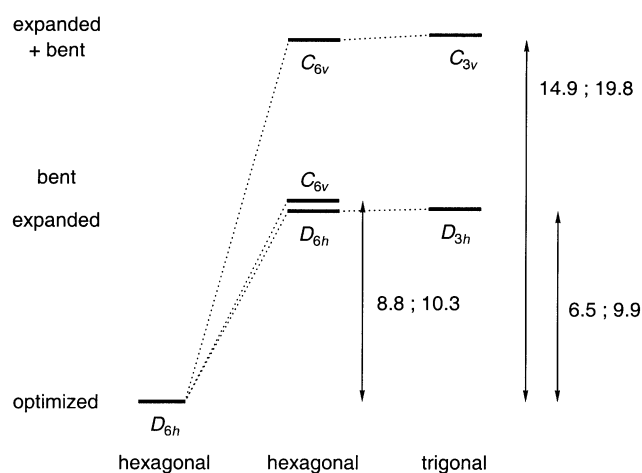


Figure 4. Relative energy of various distorted structures of benzene. Energy differences are given in kcal mol⁻¹ (B3LYP/6–311 + G**; MP2/6–311 + G**) relative to the optimized (B3LYP/6–311 + G**//B3LYP/6–311 + G**; MP2/6–311 + G**//B3LYP/6–311 + G**) structure.

Table 3. Comparison of observed and calculated geometric parameters (distances [Å] and angles [°]) for some complexes $[(\text{C}_5\text{H}_5)\text{M}]_3(\mu_3\text{-C}_6\text{H}_6)$.

| | $[(\text{C}_5\text{H}_5)\text{Co}]_3(\text{C}_6\text{H}_6)$ (1a) calculated ^[c] | $[(\text{C}_5\text{H}_5)\text{Co}]_3(\text{arene})$ ^[a] experimental | $[(\text{C}_5\text{H}_5)\text{Rh}]_3(\text{C}_6\text{H}_6)$ (2) calculated ^[c] | $[(\text{C}_5\text{H}_5)\text{Rh}]_3(\text{C}_6\text{H}_6)$ (2) ^[b] experimental | $[(\text{C}_5\text{H}_5)\text{Ir}]_3(\text{C}_6\text{H}_6)$ 3 calculated ^[c] |
|--|--|--|---|---|---|
| M–M | 2.460 | 2.501 | 2.655 | 2.625 | 2.680 |
| M–C | 2.051 | 2.028 | 2.182 | 2.152 | 2.160 |
| $\eta\text{-C-C}$ | 1.444 | 1.420 | 1.441 | 1.424 | 1.455 |
| C–C | 1.460 | 1.448 | 1.467 | 1.453 | 1.483 |
| all CC | 1.452 | 1.434 | 1.454 | 1.439 | 1.469 |
| $\text{M}_3\text{-C}_6$ ^[d] | 1.92 | 1.89 | 2.04 | 2.01 | 2.02 |
| angle C–H/ C_6 | 16 | 13–18 | 16 | 19 | 20 |

[a] Weighted means of the structures in Table 1. [b] Weighted means obtained from a crystal structure analysis.^[2] [c] B3LYP/LANL2DZ + ECP. [d] Perpendicular distance between the ring planes.

optimized structure (D_{6h} , $d_{CC} = 1.394 \text{ \AA}$) to resemble the size of the facial ligand in the cluster complexes (D_{6h} , d_{CC} fixed at 1.440 \AA) is about as costly as an out-of-plane distortion of the C–H bonds by 17° , both at the B3LYP/6–311 + G**//B3LYP/6–311 + G** and MP2/6–311 + G**//B3LYP/6–311 + G** levels. The energetic effects are roughly additive (the simultaneously expanded and bent structure has the highest energy, about twice as much as from expansion or C–H bending alone). A further trigonal distortion of the expanded planar and nonplanar molecules, respectively, to give the D_{3h} and C_{3v} Kekulé structures with d_{CC} fixed at 1.430 , 1.450 \AA , causes only a very small increase (less than $0.2 \text{ Kcal mol}^{-1}$ both at the B3LYP and MP2 levels of theory) of the total energy. Hence, as far as the total energy is concerned, C–C bond alternation in the order of magnitude as observed in the title complexes is irrelevant.

Cyclic electron delocalization: Now turning to the question of aromaticity of the facially-coordinated arenes, we first have to pay tribute to the elusive character of this very property. Not wishing to indulge ourselves in joining the ongoing passionate discussion on this subject,^[23] we merely note that despite the frequent use of the term aromaticity in the past and present literature it is not a measurable quantity and can be described by several, not necessarily correlated parameters. To overcome the more historical meanings of aromaticity, cyclic electron delocalization (CED) has been suggested as a better descriptive name.^[24] In the following, we shall mainly use this more innocent term for the phenomenon in question.

Traditionally, geometry-based indices of aromaticity have been playing an important role.^[25] With respect to our problem, in some early reports, researchers were tempted to interpret the geometric particularities of the facial coordination mode in terms of the arene “being bonded as a triene to the metal cluster,” with an implied loss or at least considerable reduction of aromatic character.^[7, 26] This proposal will be addressed in due course.

Magnetic criteria are another cornerstone of popular aromaticity scales.^[27] Bulk magnetic effects, for example magnetic susceptibility exaltation and anisotropy, and magnetic shieldings, for example as measured by NMR spectroscopy, are somehow associated with and perhaps caused by ring currents,^[28] which themselves may be thought of as directly resulting from CED. To avoid the ubiquitous problem of a suitable reference system, Schleyer et al. proposed an additional magnetic criterion for CED: nucleus independent chemical shift (NICS).^[29] NICS is readily available from

quantum-mechanical calculations at various levels of theory, but is also affected by the local effects of σ bonds and lone pairs. Using an analysis based on the IGLO method,^[30] it has been shown that the total NICS of benzene (and related molecules) at a particular point in space may be dissected into paratropic and diatropic components, which mainly arise from the C–C σ and π multiple bonds, respectively.^[31] The paratropic C–C(σ) effects fade out more rapidly with increasing distance from the ring centroid than the diatropic C–C(π) contributions. In the absence of a detailed analysis of the individual contributions of bonds, lone pairs and core electrons NICS(1) (at 1 \AA above the ring centroid) is recommended as a CED diagnostic.^[32] NICS may be mapped in three-dimensional space;^[33] significantly negative NICS values along the direction normal to a ring system indicate the presence of induced diatropic ring currents, a characteristic of CED.

NICS has been calculated for a wide range of organic π -systems. NICS indices derived from density functional calculations have also been reported for a few organotransition metal complexes, notably $[(\text{CO})_3\text{Cr}(\eta^6\text{-C}_6\text{H}_6)]$ **4** and $[\text{Cr}(\eta^6\text{-C}_6\text{H}_6)_2]$. The values obtained from calculations at the PW91 IGLO/III TZ2P level (e.g. first column in Table 4) were taken as an indication that there is no disruption of the ring current of benzene on complexation.^[34]

One goal of the present study was to make comparisons throughout the series **1–3**. It was therefore essential to employ the same orbital basis set for all the model complexes. Calculations with large all-electron basis sets are of course very costly, and even self-forbidden for the heavier metals Rh and Ir. To evaluate the effects of smaller basis sets and effective core potentials (ECP) on NICS of metal coordinated benzene, preliminary calculations were carried out on complex **4**. Our results are summarized in Table 4. Taking NICS(1) as the critical value, and the data reported by Schleyer et al.^[34] as a reference, it can be seen that nothing is gained in going beyond the 6–311G* basis with the B3LYP functional. Although it is clearly inappropriate for the calculation of magnetic properties in the vicinity of the metal, the LANL2DZ (+ECP for Cr) basis performs quite well for our purpose, and was therefore adopted for most further calculations.

NICS values were calculated for the μ_3 -benzene and η^5 -cyclopentadienyl rings in the cluster complexes $[(\eta\text{-C}_5\text{H}_5)\text{M}]_3(\mu_3\text{-}\eta^2\text{:}\eta^2\text{:}\eta^2\text{-C}_6\text{H}_6)$ **1a**, **2** and **3** (Table 5). The data obtained for **1a** with the B3LYP/6–311G** theoretical model are quite similar to those calculated with B3LYP/

Table 4. Computed NICS(d) indices for $[(\text{CO})_3\text{Cr}(\eta^6\text{-C}_6\text{H}_6)]$ **4** in the centre of the η^6 -benzene and d [\AA] above, calculated with various theoretical methods. The geometry was optimized at the B3LYP/6–311G* level.

| d [\AA] | PW91 IGLO/III TZ2P ^[a] | HF/6–311G** | B3LYP/6–311G* | B3LYP/6–311G** | B3LYP/6–311 + G** | B3LYP/LANL2DZ + ECP |
|----------------------|-----------------------------------|-------------|---------------|----------------|-------------------|---------------------|
| 3.0 | –1.0 (0.3) | –2.2 | –1.4 | –1.4 | –1.4 | –1.8 |
| 2.5 | –1.8 (0.0) | –3.6 | –2.3 | –2.4 | –2.4 | –2.8 |
| 2.0 | –3.5 (–0.9) | –6.1 | –4.1 | –4.2 | –4.2 | –4.7 |
| 1.5 | –7.0 (–3.3) | –11.0 | –7.6 | –7.7 | –8.0 | –8.0 |
| 1.0 | –13.2 (–9.3) | –19.0 | –13.5 | –13.6 | –14.4 | –13.2 |
| 0.5 | –20.1 (–17.7) | –28.6 | –20.1 | –20.2 | –21.1 | –18.2 |
| 0.0 | –25.8 (–23.2) | –40.4 | –27.0 | –27.2 | –27.8 | –24.1 |

[a] Given as total NICS with the C–C(π) contributions in parentheses; geometry at B3LYP/6–311 + G** (data from ref. [34]).

Table 5. Computed NICS(*d*) indices for $[(C_5H_5)_3M](\mu_3-C_6H_6)$ **1a–3** in the centre of the μ_3 -benzene and *d* [Å] above. The geometries were optimized at the B3LYP/LANL2DZ + ECP level.

| <i>d</i> [Å] | 1a (M = Co) B3LYP/LANL2DZ + ECP | | 1a (M = Co) B3LYP/6–311G** | | 2 (M = Rh) B3LYP/LANL2DZ + ECP | | 3 (M = Ir) B3LYP/LANL2DZ + ECP | |
|--------------|---|---------------|--------------------------------------|---------------|--|---------------|--|---------------|
| | $\mu_3-C_6H_6$ | $\eta-C_5H_5$ | $\mu_3-C_6H_6$ | $\eta-C_5H_5$ | $\mu_3-C_6H_6$ | $\eta-C_5H_5$ | $\mu_3-C_6H_6$ | $\eta-C_5H_5$ |
| 3.0 | –0.8 | –1.4 | –0.4 | –1.4 | –0.6 | –1.3 | –0.4 | –1.2 |
| 2.5 | –1.3 | –2.4 | –0.8 | –2.4 | –0.9 | –2.1 | –0.6 | –2.0 |
| 2.0 | –2.2 | –4.1 | –1.8 | –4.3 | –1.6 | –3.5 | –1.0 | –3.5 |
| 1.5 | –4.1 | –7.1 | –3.9 | –8.1 | –3.0 | –5.9 | –1.9 | –6.1 |
| 1.0 | –7.9 | –12.6 | –8.0 | –14.7 | –5.7 | –10.2 | –4.0 | –10.9 |
| 0.5 | –13.9 | –20.3 | –14.5 | –23.7 | –9.7 | –15.8 | –7.6 | –17.1 |
| 0.0 | –20.0 | –27.1 | –22.3 | –32.7 | –12.4 | –18.5 | –10.1 | –19.5 |

LANL2DZ + ECP, again illustrating that this small-core ECP basis is quite suitable for our problem. Variation of NICS with the distance *d* perpendicular to the benzene ring plane is shown in Figure 5, along with our data for the mononuclear

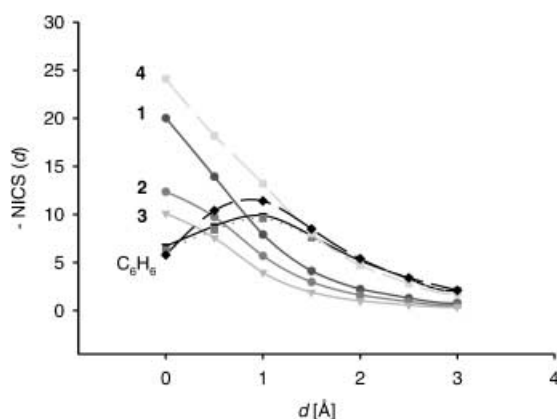


Figure 5. NICS(*d*) indices in the centre of the benzene rings and *d* Å above for three geometries of benzene (solid: hexagonal, $d_{CC}=1.394$ Å; dotted: trigonal, $d_{CC}=1.430, 1.450$ Å; dashed: trigonal with CH bonds out of plane), $[(CO)_3Cr(\eta^6-C_6H_6)]$ **4** and $\mu_3-\eta^2:\eta^2:\eta^2$ -benzene in the complexes $[(C_5H_5)_3M](\mu_3-C_6H_6)$ **1a–3** (M = Co, Rh, Ir).

η^6 -benzene complex **4** and for free benzene with an undistorted (optimized, $d_{CC}=1.394$ Å) or expanded and slightly distorted frame ($d_{CC}=1.430, 1.450$ Å, planar and with the CH bonds bent out of plane), respectively. NICS(*d*) indices for the cyclopentadienyl rings in the cluster complexes are visualized in Figure 6. From Figure 5, it is immediately evident that expansion and Kekulé distortion of free benzene in the order of magnitude as observed in **1** does not have an influence on NICS and hence on CED. The maximum around $d=1$ Å in the curves for free benzene is due to the substantial paratropic contribution of C–C(σ), which counteracts the π -effects near the centroid of the ring.^[31] The somewhat higher NICS values at $d \leq 1.5$ Å for the nonplanar structure are due to the closer vicinity of the CH bonds, which have a diatropic effect.^[31] σ -Effects are small in the mononuclear benzene complex **4** (Table 4), resulting in a monotonously falling curve for NICS.^[34] Judging from the shape of the NICS curves this is also the case for both the $\eta^5-C_5H_5$ and $\mu_3-\eta^2:\eta^2:\eta^2-C_6H_6$ ligands in the cluster complexes **1a**, **2** and **3**. Compared to η^5 -cyclopentadienyl and to η^6 -benzene, calculated NICS are always smaller for the $\mu_3-\eta^2:\eta^2:\eta^2$ -benzene ligand. Consistent with the ring–metal(s) interaction becoming stronger, de-

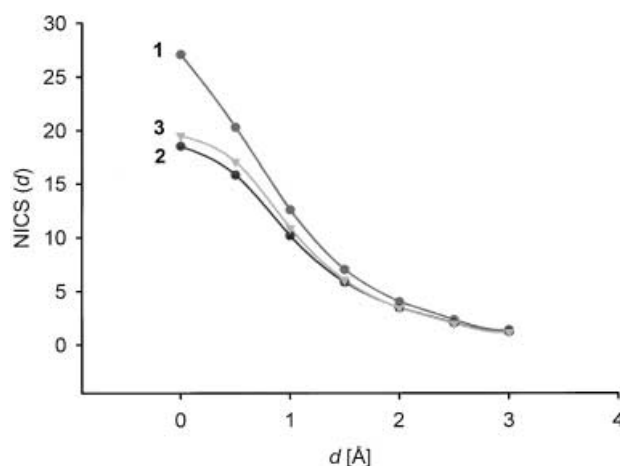


Figure 6. NICS(*d*) indices in the center of the cyclopentadienyl rings and *d* Å above in complexes of the type $[(C_5H_5)_3M](\mu_3-C_6H_6)$ **1a–3** (M = Co, Rh, Ir)

scending the cobalt group of the periodic table also leads to a reduction of NICS for both ligands in the corresponding cluster complexes. NICS(1) indices for μ_3 -benzene of about –8 (M = Co), –6 (M = Rh) and –4 (M = Ir) however still indicate substantial CED, but definitely less than in the cyclopentadienyl rings or in the η^6 -benzene in **4**.

NMR chemical shifts: NICS is not an observable property. To evaluate the reliability of our NICS calculations we have also calculated 1H and ^{13}C NMR chemical shifts for the facial benzene and apical cyclopentadienyl ligands.^[35] A comparison with experimental data is compiled in Table 6. The observed trend upon facial complexation of benzene—a strong high-field shift of the carbon and proton resonances—is nicely

Table 6. A comparison of calculated vs. experimental ^{13}C and 1H NMR chemical shifts^[a] (δ) for benzene and $[(C_5H_5)_3M](\mu_3\text{-arene})$ **1–3**.

| Compd | Basis | C_6H_6 | C_6H_6 | C_5H_5 | C_5H_5 |
|------------------------------|----------|----------------------|----------|----------|----------|
| benzene calcd ^[b] | 6–311G** | 134.0 | 7.5 | | |
| benzene exptl | | 128.7 | 7.4 | | |
| 1a calcd | 6–311G** | 47.3–47.9 | 4.1–4.3 | 88.0 | 4.6 |
| | LANL2DZ | 46.3–48.1 | 3.9–4.0 | 89.0 | 5.3 |
| 1b–m exptl | | 39–45 ^[c] | 4.2–4.6 | 81–83 | 4.5–4.9 |
| 2 calcd | LANL2DZ | 53.4–54.9 | 4.1–4.3 | 92.6 | 5.7 |
| 2 exptl | | | 4.1 | | 5.1 |
| 3 | LANL2DZ | 42.4–45.4 | 3.3–3.5 | 88.0 | 5.4 |

[a] Relative to Si(Me)₄. [b] Geometry optimized at the B3LYP/6–311G** level. [c] CH groups.

reproduced by the calculations. Calculated carbon chemical shifts for the trirhodium complex **2** are consistently larger on the δ scale (i.e. less shifted with respect to free benzene) than for both the cobalt and iridium complexes **1** and **3**. Unfortunately, since experimental carbon NMR data for **2** have not been reported, comparison with experimental data is restricted to the cobalt series only. Given the fact that the ordering of carbon chemical shifts is $\delta(\text{Rh}) > \delta(\text{Co}) > \delta(\text{Ir})$ in many organometallic complexes of the cobalt group metals^[36] our calculated values do not appear unreasonable.

Conclusion

With respect to the bonding described above “as a triene” of the facial benzene we consider the observed and calculated C–C bond length alternation in the order of $\Delta d = 0.03 \text{ \AA}$ insufficient by far to warrant such an extreme picture of the bonding. It should be noted here that a quite similar deviation from sixfold symmetry, but with a somewhat less pronounced expansion of the ring, was found in the centrally η^6 -bonded benzene ligand of **4** [$d_{\text{CC}} = 1.406(2), 1.423(2) \text{ \AA}$ (X-ray and neutron structures);^[37] $1.406(4), 1.422(4) \text{ \AA}$ (microwave structure)^[38]]. The electronic reasons for these small distortions are similar and well understood for both η^6 - and μ_3 -benzene.^[21, 39, 40]

In free benzene, bond length alternation correlates with NICS.^[41] However, even a strong Kekulé distortion only results in a relatively small reduction of diatropic NICS.^[29, 41] NICS indices calculated for benzene with d_{CC} fixed at 1.420, 1.450 \AA (as in the prototypal μ_3 - η^2 : η^2 : η^2 -benzene ligand) are essentially the same as for regular benzene (Figure 5). CED drops in the series free benzene $\approx \eta^6$ -benzene $> \mu_3$ - η^2 : η^2 : η^2 -benzene, but still with substantial CED left in the cluster-coordinated facial benzene. Evidently, the moderate diminution of CED in the facial benzene ligand does not result in a corresponding Kekulé-type distortion that is nearly as large. In other words, μ_3 - η^2 : η^2 : η^2 coordination of benzene to a trinuclear transition-metal cluster reduces CED more than would be expected from the trigonal distortion of the facial ligand itself. However, CED is still far from being quenched completely.

Acknowledgement

This work was supported by the Forschungsschwerpunktprogramm (Baden-Württemberg) “Modellierung von Moleküleigenschaften als grundlegende Methodik moderner Molekülchemie” and by the Graduiertenkolleg 850 “Modellierung von Moleküleigenschaften”. We thank Prof. M. J. Calhorda (ITQB Oeiras and Universidade de Lisboa) for helpful discussions and for her hospitality at ITQB. Support from the European Union (ERASMUS) and a travel grant by the Deutscher Akademischer Austauschdienst is gratefully acknowledged.

- [1] H. Wadepohl, K. Büchner, M. Herrmann, A. Metz, H. Pritzkow, *J. Organomet. Chem.* **1998**, 571, 267.
 [2] Review articles: a) H. Wadepohl, *Angew. Chem.* **1992**, 104, 253; *Angew. Chem. Int. Ed. Engl.* **1992**, 31, 247; b) D. Braga, P. J. Dyson, F. Grepioni, B. F. G. Johnson, *Chem. Rev.* **1994**, 94, 1585; c) H. Wadepohl, S. Gebert, *Coord. Chem. Rev.* **1995**, 143, 535; d) H. Wadepohl, A.

- Metz in *Metal Clusters in Chemistry, Vol. 1* (Eds.: P. Braunstein, L. A. Oro, P. R. Raithby), Wiley-VCH, Weinheim **1999**, Ch. 1.15.
 [3] H. Wadepohl in *Physical Organometallic Chemistry Vol. 3* (Eds.: M. Gielen, R. Willem, B. Wrackmeyer), Wiley, Chichester **2002**, 297.
 [4] See, for example: F. P. Netzer, *Langmuir* **1991**, 7, 2544, and references therein.
 [5] a) G. A. Somorjai, U. Starke, *Pure Appl. Chem.* **1992**, 64, 509; b) G. A. Somorjai, *J. Phys. Chem. B* **2000**, 104, 2969.
 [6] F. P. Netzer, M. G. Ramsey, *Crit. Rev. Solid State Mater. Sci.* **1992**, 17, 397, and references therein.
 [7] B. F. G. Johnson, J. Lewis, C. Housecroft, M. Gallop, M. Martinelli, D. Braga, F. Grepioni, *J. Molec. Catal.* **1992**, 74, 61.
 [8] a) *Appl. Statist.*, algorithms AS66 (**1973**, 22(3)); AS111 (**1977**, 26(1)); AS177, 177.1, AS177.2, AS177.3, AS177.4 (**1982**, 31(2)); AS181, AS181.1, AS181.2 (**1982**, 31(2)); b) *Numerical Recipes in Fortran-77: The Art of Scientific Computing*, Cambridge University Press, Cambridge **1986**, Ch. 14; c) *STARPA User's Guide*, J. R. Donaldson, P. V. Tryon, U. S. Department of Commerce, Center for Computing and Applied Mathematics, National Institute of Standards and Technology, Boulder, Co., USA, Internal Report NBSIR 86–3448, **1990**; d) R. Taylor, F. H. Allen in *Structure Correlation* (Eds.: H.-B. Bürgi, J. Dunitz), VCH, Weinheim **1994**, Vol. 1, Ch. 4.
 [9] W. Koch, M. C. Holthausen, *A Chemist's Guide to Density Functional Theory*, Wiley-VCH, Weinheim, 2nd ed. **2001**.
 [10] M. J. Frisch, G. W. Trucks, H. B. Schlegel, G. E. Scuseria, M. A. Robb, J. R. Cheeseman, V. G. Zakrzewski, J. A. Montgomery, Jr., R. E. Stratmann, J. C. Burant, S. Dapprich, J. M. Millam, A. D. Daniels, K. N. Kudin, M. C. Strain, O. Farkas, J. Tomasi, V. Barone, M. Cossi, R. Cammi, B. Mennucci, C. Pomelli, C. Adamo, S. Clifford, J. Ochterski, G. A. Petersson, P. Y. Ayala, Q. Cui, K. Morokuma, D. K. Malick, A. D. Rabuck, K. Raghavachari, J. B. Foresman, J. Cioslowski, J. V. Ortiz, B. B. Stefanov, G. Liu, A. Liashenko, P. Piskorz, I. Komaromi, R. Gomperts, R. L. Martin, D. J. Fox, T. Keith, M. A. Al-Laham, C. Y. Peng, A. Nanayakkara, C. Gonzalez, M. Challacombe, P. M. W. Gill, B. Johnson, W. Chen, M. W. Wong, J. L. Andres, C. Gonzalez, M. Head-Gordon, E. S. Replogle, J. A. Pople, *Gaussian 98*, Rev. A.6, Gaussian, Inc., Pittsburgh PA, **1998**.
 [11] P. J. Hay, W. R. Wadt, *J. Chem. Phys.* **1985**, 82, 299.
 [12] J. R. Cheeseman, G. W. Trucks, T. A. Keith, M. J. Frisch, *J. Chem. Phys.* **1996**, 104, 5497, and references therein.
 [13] H. Wadepohl in *The Synergy Between Dynamics and Reactivity at Clusters and Surfaces* (Ed.: L. J. Farrugia), *NATO ASI Series C: Mathematical and Physical Sciences*, Vol. 465, Kluwer, Dordrecht **1995**, p. 175.
 [14] W. M. Harper, *Statistics*, Macdonald and Evans, Estover **1977**, Part 6, Ch. 19–24.
 [15] a) M. B. Wilk, R. Gnanadesikan, *Biometrika* **1968**, 55, 1; b) S. C. Abrahams, E. T. Keve, *Acta Crystallogr. Sect. A* **1971**, 27, 157; c) W. C. Hamilton, *Acta Crystallogr. Sect. A* **1972**, 28, 215.
 [16] a) J. P. Royston, *Appl. Statist.* **1982**, 31, 115; J. P. Royston, *Appl. Statist.* **1982**, 31, 176; J. P. Royston, *Appl. Statist.* **1986**, 35, 232.
 [17] a) A. Domenicano, A. Vacigo, C. A. Coulson, *Acta Crystallogr. Sect. B* **1975**, 31, 221; b) A. Domenicano in *Accurate Molecular Structures, IUCr Monographs on Crystallography Vol. 1* (Eds.: A. Domenicano, I. Hargittai), International Union of Crystallography and Oxford University Press, Oxford **1992**, Ch. 18.
 [18] R. Taylor, O. Kennard, *Acta Crystallogr. Sect. B* **1986**, 42, 112.
 [19] R. Taylor, O. Kennard, *Acta Crystallogr. Sect. A* **1985**, 41, 85.
 [20] J. Müller, P. Escarpa Gaede, K. Qiao, *Angew. Chem.* **1993**, 105, 1809; *Angew. Chem. Int. Ed. Engl.* **1993**, 32, 1697.
 [21] a) H. Wadepohl, L. Zhu, *J. Organomet. Chem.* **1989**, 376, 115; b) L. Zhu, H. Wadepohl, N. Kostic, *Wuji Huaxue Xuebao* **1992**, 8, 1.
 [22] H. Wadepohl, M. J. Calhorda, M. Herrmann, C. Jost, P. E. M. Lopes, H. Pritzkow, *Organometallics* **1996**, 15, 5622.
 [23] An entire issue of *Chemical Reviews* (*Chem. Rev.* **2001**, 101(5)), special issue editor: P. von R. Schleyer; editorial: P. von R. Schleyer, *Chem. Rev.* **2001**, 101, 1115) has recently been devoted to aromaticity. This authoritative collection of review articles is highly commendable.
 [24] P. v. R. Schleyer, H. Jiao, *Pure Appl. Chem.* **1996**, 68, 209.
 [25] T. M. Krygowski, M. K. Cyrański, *Chem. Rev.* **2001**, 101, 1385, and references therein.

- [26] M. P. Gomez-Sal, B. F. G. Johnson, J. Lewis, P. R. Raithby, A. H. Wright, *J. Chem. Soc. Chem. Commun.* **1985**, 1682.
- [27] R. C. Benson, W. H. Flygare, *J. Am. Chem. Soc.* **1970**, *92*, 7593.
- [28] a) P. W. Fowler, E. Steiner, *J. Phys. Chem. A* **1997**, *101*, 1409, and references therein; b) P. Lazzaretti, *Progr. Nucl. Magn. Reson.* **2000**, *36*, 1, and references therein; c) J. A. N. F. Gomes, R. B. Mallion, *Chem. Rev.* **2001**, *101*, 1349, and references therein.
- [29] P. von R. Schleyer, C. Maerker, A. Dransfeld, H. Jiao, N. J. R. van Eikema Hommes, *J. Am. Chem. Soc.* **1996**, *118*, 6317.
- [30] W. Kutzelnigg, U. Fleischer, M. Schindler in *NMR Basic Principles and Progress Vol. 23* (Eds.: P. Diehl, E. Fluck, H. Günther, R. Kosfield, J. Seeling), Springer, Heidelberg **1990**.
- [31] P. von R. Schleyer, M. Manoharan, Z.-X. Wang, B. Kiran, H. Jiao, R. Puchta, N. J. R. v. Eikema Hommes, *Org. Lett.* **2001**, *3*, 2465.
- [32] P. von R. Schleyer, H. Jiao, N. J. R. v. Eikema Hommes, V. G. Malkin, O. L. Malkina, *J. Am. Chem. Soc.* **1997**, *119*, 12669.
- [33] a) S. Klod, E. Kleinpeter, *J. Chem. Soc. Perkin Trans. 2*, **2001**, 1893; b) S. Klod, A. Koch, E. Kleinpeter, *J. Chem. Soc. Perkin Trans. 2*, **2002**, 1506.
- [34] P. von R. Schleyer, B. Kiran, D. V. Simion, T. S. Sorensen, *J. Am. Chem. Soc.* **2000**, *122*, 510.
- [35] It should be noted here that Pople's ring current model (J. A. Pople, *J. Chem. Phys.* **1956**, *24*, 1111; *Mol. Phys.* **1958**, *1*, 175) has been shown to be inadequate to explain the "anomalous" (downfield) NMR chemical shifts of peripheral protons in aromatic ring systems: U. Fleischer, W. Kutzelnigg, P. Lazzaretti, V. Mühlkamp, *J. Am. Chem. Soc.* **1994**, *116*, 5298; C. S. Wannere, P. von R. Schleyer, *Org. Lett.* **2003**, *5*, 605.
- [36] B. E. Mann, B. F. Taylor, *¹³C NMR Data for Organometallic Compounds*, Academic Press, London **1981**.
- [37] B. Rees, P. Coppens, *Acta Crystallogr. Sect. B* **1973**, *29*, 2515.
- [38] S. G. Kukolich, *J. Am. Chem. Soc.* **1995**, *117*, 5512.
- [39] A. L. Low, M. B. Hall, *Int. J. Quant. Chem.* **2000**, *77*, 152.
- [40] J.-F. Riehl, N. Koga, K. Morokuma, *Organometallics* **1993**, *12*, 4788.
- [41] M. K. Cyrański, T. M. Krygowski, *Tetrahedron* **1999**, *55*, 6205.

Received: February 21, 2003
Revised: July 2, 2003 [F4875]